

Modeling the gamma-ray emission produced by runaway cosmic rays in the environment of RX J1713.7-3946

Sabrina CASANOVA¹, David I. JONES¹, Felix A. AHARONIAN^{1,2}, Yasuo FUKUI³, Stefano GABICI^{2,4}, Akiko KAWAMURA³, Toshikazu ONISHI³, Gavin ROWELL⁵, Hidetoshi SANO³, Kazufumi TORII³, Hiroaki YAMAMOTO³

¹*Max Planck für Kernphysik, Saupfercheckweg 1, 69117, Heidelberg*

²*Dublin Institute for Advance Physics, 31 Fitzwilliam Place, Dublin 2, Ireland*

³*Nagoya University, Furo-cho, Chikusa-ku, Nagoya City, Aichi Prefecture, Japan*

⁴*Laboratoire APC, 10, rue Alice Domon et Léonie Duquet, 75013 Paris, France*

⁵*School of Chemistry and Physics, University of Adelaide, Adelaide 5005, Australia*

(Received ; accepted)

Abstract

Diffusive shock acceleration in supernova remnants is the most widely invoked paradigm to explain the Galactic cosmic ray spectrum. Cosmic rays escaping supernova remnants diffuse in the interstellar medium and collide with the ambient atomic and molecular gas. From such collisions gamma-rays are created, which can possibly provide the first evidence of a parent population of runaway cosmic rays. We present model predictions for the GeV to TeV gamma-ray emission produced by the collisions of runaway cosmic rays with the gas in the environment surrounding the shell-type supernova remnant RX J1713.7-3946. The spectral and spatial distributions of the emission, which depend upon the source age, the source injection history, the diffusion regime and the distribution of the ambient gas, as mapped by the LAB and NANTEN surveys, are studied in detail. In particular, we find for the region surrounding RX J1713-3946, that depending on the energy one is observing at, one may observe startlingly different spectra or may not detect any enhanced emission with respect to the diffuse emission contributed by background cosmic rays. This result has important implications for current and future gamma-ray experiments.

Key words: ISM: clouds, ISM: cosmic rays, ISM: supernova remnants, gamma rays: theory

1. Introduction

Cosmic rays (CRs) are the highly energetic protons and nuclei which fill the Galaxy and carry, at least in the vicinity of the Sun, as much energy per unit volume as the energy density of starlight or of the interstellar magnetic fields or the kinetic energy density of the interstellar gas.

CRs of energies up to the “knee” (10^{15} eV), or even up to 10^{18} eV, are believed to originate from sources located within the Galaxy. Galactic CRs are thought to be accelerated via diffusive shock acceleration (DSA) operating in the expanding shells of supernova remnants (SNRs). For references see e.g. Blandford & Eichler 1987 ; Malkov & Drury 2001 . The accelerated CRs interact with ambient gas through inelastic collisions, producing neutral pions, which then decay into γ -rays .

If the bulk of Galactic CRs up to at least PeV energies are indeed accelerated in SNRs, then TeV γ -rays are expected to be emitted during the acceleration process CRs undergo within SNRs (Drury, Aharonian & Völk 1994). Indeed TeV γ -rays have been detected from the shells of SNRs (Aharonian et al. 2006 ; Albert et al. 2007b). However, such observations do not constitute a definitive proof that CRs are accelerated in SNRs, since the observed emission could be produced by energetic electrons up scattering low energy photon fields. We note, in fact, that γ -rays are also produced through inverse Compton and bremsstrahlung processes of very highly energetic electrons.

γ -rays are also expected to be emitted when the accelerated CRs propagate into the interstellar medium (ISM) (Montmerle 1979 ; Issa & Wolfendale 1981 ; Aharonian 1991 ; Aharonian & Atoyan 1996 ; Gabici, Aharonian & Casanova 2009). Before being isotropised by the Galactic magnetic fields, the injected CRs produce γ -ray emission, which can significantly differ from the emission of the SNR itself, as well as from the diffuse emission contributed by the background CRs and electrons, because of the hardness of the runaway CR spectrum, which is not yet steepened by diffusion. The extension of such diffuse sources does not generally exceed a few hundred parsecs, the scale at which the spectra of the injected CRs can significantly differ from the spectrum of the CR background (Aharonian & Atoyan 1996 ; Gabici & Aharonian 2007 ; Rodriguez Marrero et al. 2008 ; Gabici, Aharonian & Casanova 2009). These diffuse sources are often correlated with dense molecular clouds (MCs), which act as a target for the production of γ -rays due to the enhanced local CR injection spectrum. Paul, Casse & Cesarsky 1976 and Montmerle 1979 have pointed out that SNRs are located in star forming regions, which are rich in molecular hydrogen. In other words, CR sources and MCs are often associated and target-accelerator systems are not unusual within the Milky Way. In fact, there have been recently claims of detection of γ -rays in association with dense MCs close to candidate CR sources, both at GeV energies (Abdo et al. 2009c ; Abdo et al. 2010 ; Tavani et al. 2010 ; Castro & Slane 2010) and TeV energies (Albert et al. 2007a ; Aharonian et al 2008a ; Aharonian et

al 2008b ; Aharonian et al 2008c).

In order to probe the interaction of the low-energy component of the ambient cosmic ray flux, Montmerle 2009 has recently proposed to measure enhanced ionization in TeV-bright molecular clouds, using millimeter observations. On the other hand, high energy CRs (above 1 GeV up to PeV energies) interacting with the ambient gas emit γ -rays . For this reason the high sensitivity, high resolution γ -ray data from current (HESS, Magic, Veritas, Fermi and Agile) and future detectors, such as AGIS, CTA and HAWC (Aharonian, Buckley, Kifune and Sinnis 2008 ; Hinton & Hofmann 2009), together with the knowledge of the distribution of the atomic and molecular hydrogen in the Galaxy on sub-degree scales are crucial to explore the flux of high energy CRs close to the candidate CR sources and to pinpoint the long searched-for sites of CR acceleration.

The γ -ray radiation from hadronic interactions from regions close to CR sources depends not only on the total power emitted in CRs by the sources and on the distance of the source to us, but also on the ambient interstellar gas density, the local diffusion coefficient and the injection history of the CR source. It is therefore difficult to definitely recognize the sites of CR acceleration from γ -ray observations alone, since very often only qualitative predictions are provided, rather than robust quantitative predictions, especially from a morphological point of view. In order to fully exploit the present and future experimental facilities and to test the standard scenario for CR injection in SNRs and propagation, we present here model predictions of the spectral and morphological features of the hadronic γ -rays emission surrounding the candidate CR source, RX J1713.7-3946, by constructing as quantitative a model as possible. In particular, we will convey all information concerning the environment, the source age, the acceleration rate and history, which all play a role in the physical process of CR injection and propagation. Building upon the modeling of the broadband emission from MCs close to CR accelerators developed in Gabici, Aharonian & Casanova 2009 and upon the analysis of the CR background discussed in Casanova et al. 2009 (hereafter Paper 1), we compute the expected γ -ray emissivity from hadronic interactions of runaway CRs for the region $340^\circ < l < 350^\circ$ and $-5^\circ < b < 5^\circ$, assuming that a historical SNR event occurred in 393 C.E., at the location of the SNR RX J1713.7-3946 (Wang, Qu & Chen 1997).

RX J1713-3946 is thought of as one of the best examples of a shell-type SNR, for which the multi-wavelength data suggests hadronic CR particle acceleration is active up to at least 100 TeVs (Aharonian et al. 2006). The acceleration site within RX J1713.7-3946 is spatially coincident with the sites of non-thermal X-ray emission and brightening and decay of the X-ray hot spots on year time-scales have been detected (Uchiyama et al. 2007). The observed rapid variability of the X-ray emission provides strong evidence for the amplification of the magnetic field around the SNR shell, which is is key condition for the acceleration of protons beyond the 100 TeV limit set by Lagage & Cesarsky 1983 . The multi-wavelength analysis of the emission from RX J1713.7-3946 supports therefore the hypothesis that CRs up to the

knee are accelerated in SNRs. However, no compelling evidence for the acceleration of protons and nuclei up to PeV energies has been found until now. Also, the most energetic CRs cannot be confined for long time within the SNR and, even if RX J1713-3946 might have accelerated particles up to about PeV energies once, such highly energetic protons have already left the source. In fact, these very energetic particles, which are released first by SNRs and diffuse faster than lower energy CRs, reach as first the clouds surrounding the injection sites and produce enhanced γ -ray emission. This is why studies of the γ -ray emission from environment surrounding RX J1713-3946, such as the one presented here, are important.

In Section 2 we will briefly describe the results of the LAB survey of the Galactic atomic hydrogen and of the NANTEN survey of the Galactic molecular clouds. Section 3 will be dedicated to the description of the model. The predictions of the model for the emission from the region under consideration are presented in Section 4, where we will also discuss the observational prospects for present and future observatories. Our conclusions are given in Section 5.

2. Survey data

The distributions of atomic and molecular hydrogen in the Galaxy, used in the following calculations, are from the Leiden/Argentine/Bonn (LAB) Galactic HI Survey (Karberla et al. 2005) and from the NANTEN Survey (Fukui et al 1999 ; Fukui et al. 2001 ; Fukui et al. 2003 ; Fukui et al. 2008), respectively.

The LAB observations of atomic hydrogen were centered on the 1420 MHz (λ 21 cm) line with a bandwidth of 5 MHz. The velocity axis spans -450 km s^{-1} to 400 km s^{-1} giving a final velocity resolution of 1.3 km s^{-1} . The data combines observations from three telescopes at a resolution of 0.6° with a final sensitivity of $\sim 0.1 \text{ K}$.

The NANTEN instrument is a 4 m millimetre/sub-millimetre telescope, which has surveyed the southern sky, using the ^{12}CO (J=1-0) emission line at 115.271 GHz ($\lambda = 2.6 \text{ mm}$). The survey was performed with an angular resolution of $4'$, with a mass sensitivity of about $100 M_\odot$ at the Galactic centre and 1 km/s resolution in velocity. From the column density of CO the column density of molecular hydrogen is obtained by assuming the conversion factor, X ,

$$X = 1.4 \times 10^{20} e^{(R/11 \text{ kpc})} [\text{cm}^{-2} \text{K}^{-1} \text{km}^{-1} \text{s}], \quad (1)$$

where R is distance to the GC (Nakanishi & Hiroiyuki 2003 ; Nakanishi & Hiroiyuki 2006).

The survey data-cubes of both atomic and molecular hydrogen, given in longitude, latitude and velocity, are transformed into data-cubes in longitude, latitude and heliocentric distance by using a flat rotation curve model of the Galaxy with uniform velocity equal to 220 km/s (Nakanishi & Hiroiyuki 2003 ; Nakanishi & Hiroiyuki 2006). In Figure 1 the three dimensional gas distribution (sum of the atomic and molecular gas) in the region which spans Galactic

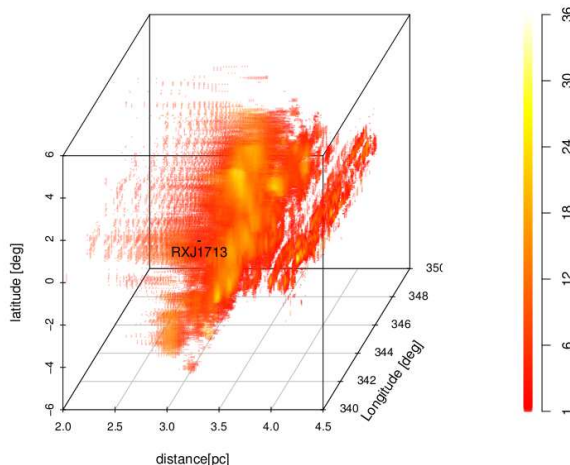


Fig. 1. The gas distribution in the region which spans Galactic longitude $340^\circ < l < 350^\circ$, Galactic latitude $-5^\circ < b < 5^\circ$ and heliocentric distance $100 \text{ pc} < l_d < 30 \text{ kpc}$, as observed by the NANTEN and LAB surveys, expressed in protons cm^{-3} . The distance axis is logarithmic in base 10. A value for the gas density is given every 50 pc in distance, which is reflected in the apparent slicy structure for distances below 100 pc. For sake of clarity only densities above 1 protons cm^{-3} are shown. Also indicated the position of the historical SNR, RX J1713.7-3946.

longitude $340^\circ < l < 350^\circ$, Galactic latitude $-5^\circ < b < 5^\circ$ and distance $100 \text{ pc} < l_d < 30 \text{ kpc}$ is shown. For a detailed discussion of the data and its limitations and errors, we refer the reader to Paper I.

3. The model

We have modeled a supernova (SN) of total energy E_{SN} , which has exploded into the ISM in the region of the Galaxy described above. Our SNR is identifiable with the historical SNR RX J1713.7-3946, is located at 1 kpc distance from the Sun and has the same coordinates as RX J1713.7-3946, i.e., $(l, b) = (347.3, -0.5)$ (Wang, Qu & Chen 1997). CRs are assumed to be injected by DSA operating at SNR shocks and the spectrum at the shock is a power law with index -2. The SNR accelerates the most energetic particles at the transition from the free expansion phase to the Sedov phase (Ptuskin and Zirakashvili 2005 ; Gabici, Aharonian & Casanova 2009 ; Caprioli, Amato & Blasi 2009). Following Gabici, Aharonian & Casanova 2009 we assume that the most energetic leave the SNR at the beginning of the Sedov phase. The particles are released at different times, depending on their energy. A particle with energy E_p escapes the SNR at a time $\chi(E_p)$, for which, following Gabici, Aharonian & Casanova 2009, we assume a power law behaviour

$$\chi(E_p) = t_{Sedov} \left(\frac{E_p}{E_{pmax}} \right)^{-1/\delta}. \quad (2)$$

The maximum injection energy in Eq. 2 is assumed to be $E_{p_{max}} = 500$ TeV. If we assume that CRs of energy $E_{p_{max}}$ and $E_p = 150$ TeV are released at an early epoch of the Sedov phase ($t = 100$ yr) and now ($t = 1600$ yr), respectively, then this requires $\delta = 0.43$. When runaway protons diffuse into the ISM, their energy density varies with energy, E_p , distance from the injection source, d , SNR age, t , and diffusion properties of the ISM (Gabici, Aharonian & Casanova 2009) as

$$\rho_{SNR}(E_p, d, t) = \frac{\eta E_{SN}}{\pi^{3/2} \ln(E_{p_{max}}/E_{p_{min}})} \times \frac{e^{-\left(\frac{d}{R_d}\right)^2}}{R_d^3} E_p^{-2}. \quad (3)$$

In Eq. 3 the fraction of the SN explosion energy, $E_{SN} = 10^{51}$ ergs, which goes into the CRs is assumed to be $\eta = 30\%$. The dependence upon the distance from the source, d , can be translated into the dependence upon the coordinates, l , b and the line of sight distance, l_d . The minimum proton energy injected is $E_{p_{min}} = 1$ GeV. In Eq. 3 R_d is the diffusion distance for a CR of energy E_p

$$R_d = \sqrt{4D(E_p)(t - \chi(E_p))} \quad (4)$$

where $\chi(E_p)$ is the time after the SN explosion at which a proton of energy E_p escapes the injection source and begins diffusing into the ISM. We also assume that the CRs released by the SNR have energy dependent diffusion coefficient

$$D(E_p) = D_0 \left[\frac{E_p}{10\text{GeV}} \right]^{0.5} \text{ cm}^2\text{s}^{-1}. \quad (5)$$

We take D_0 to be 10^{26} , 10^{27} or 10^{28} cm^2/s . The diffusion of CRs into molecular clouds depends upon the highly uncertain diffusion coefficient. It is thought that CRs can penetrate clouds if the diffusion coefficient inside the cloud is the same as the average diffusion coefficient in the Galaxy, as derived from spallation measurements. CRs are effectively excluded if the diffusion coefficient is suppressed compared to the surroundings. However, it has been shown that CRs at TeV energies can diffuse into even the densest parts of molecular clouds, whilst GeV energy CRs might have trouble penetrating the densest parts of molecular clouds (Gabici, Aharonian & Blasi 2007 ; Protheroe et al. 2008 ; Jones et al. 2009 ; Gabici, Aharonian & Casanova 2009).

3.1. Hadronic γ -ray emissivity

The hadronic γ -ray emissivity, which is given as the γ -rays produced by CRs interacting with the gas per cubic centimeter per second per GeV at a position defined by its coordinates, l , b and heliocentric distance, l_d , can be expressed as

$$e_\gamma(E_\gamma, l, b, l_d) = \frac{dN_\gamma}{dV dE_\gamma dt} = \int_{E_{pth}}^{E_{pmax}} dE_p \frac{d\sigma_{p \rightarrow \gamma}}{dE_p}(E_p, E_\gamma) c n(l, b, l_d) \rho_{CR}(E_p, l, b, l_d), \quad (6)$$

where the integral is calculated over the energy, E_p , of the protons. E_{pth} is the minimum proton energy that contributes to the production of a photon of energy E_γ . In Eq. 6 the spectral dependence of the photons emitted by CR protons, expressed in terms of the differential cross section, $d\sigma_{p \rightarrow \gamma}/dE_p$, can be calculated using the simple but precise parametrisation developed by Kelner, Aharonian & Bugayov 2006 . However, at low energies when a broad variety of proton spectra are expected, we use the parametrization by Kamae et al. 2006 . In Eq.6 c is the velocity of light and $n(l, b, l_d)$ is the ambient gas density as function of b , l and l_d . $\rho_{CR}(E_p, l, b, l_d)$ is the proton energy density, which is given by the sum of the background CR density, $\rho_{bg}(E_p)$, and the density of cosmic rays released by the SNR and diffusing into the ISM, $\rho_{SNR}(E_p, l, b, l_d)$, as given in Eq.3

$$\rho_{CR}(E_p, l, b, l_d) = \rho_{bg}(E_p) + \rho_{SNR}(E_p, l, b, l_d). \quad (7)$$

The CR background spectrum is equal to the CR flux measured at the top of the Earth's atmosphere. Below 10^6 GeV we here adopt the value of

$$\Phi_{bg}(E_p) = 1.8 \left(\frac{E_p}{\text{GeV}} \right)^{-2.7} \text{cm}^{-2} \text{s}^{-1} \text{sr}^{-1} \text{GeV}^{-1}, \quad (8)$$

taken from the Particle Data Group 2008 . A change in the spectral index of the measured CR flux is observed above 10^6 GeV, which we do not consider here since we are only interested in the γ -ray emission below 100 TeV. The background CR energy density is then defined as

$$\begin{aligned} \rho_{bg}(E_p) &= \frac{4\pi}{c} \Phi_{bg}(E_p) \\ &\simeq 7.5 \times 10^{-10} \frac{E_p}{\text{GeV}}^{-2.7} \text{cm}^{-3} \text{GeV}^{-1}. \end{aligned} \quad (9)$$

A multiplication factor of 1.5 is applied to the CR density in Eq.7, which accounts for the contribution to the emission from heavier nuclei both in CRs and in the interstellar medium (Dermer 1986 ; Mori 1997). We note that recently Mori 2009 has recalculated the multiplication factor obtaining a 20 per cent higher value.

The differential photon spectrum measured at Earth is then obtained by integrating the emissivity $e_\gamma(E_\gamma, l, b, l_d)$ over the line of sight distance l_d

$$\frac{dN_\gamma}{dAdE_\gamma dt d\Omega} = \frac{1}{4\pi} \int_0^{l_dmax} dl_d e_\gamma(E_\gamma, l, b, l_d) \quad (10)$$

3.2. *Leptonic emission from primary and secondary electrons*

γ -rays are also produced through inverse Compton and bremsstrahlung processes of very highly energetic primary and secondary electrons and positrons.

A population of primary electrons is accelerated by and confined within the SNR. The high energy primary electrons suffer, in fact, from strong losses through synchrotron emission, triggered by the amplified magnetic field of the SNR shock, while the low energy part of the primary leptonic population cannot escape due to diffusive confinement.

Inverse Compton (IC) scattering of background CR electrons results in a non-negligible contribution to the overall diffuse gamma-ray emission at GeV, and also at TeV energies, especially at high Galactic latitudes. At low latitudes the relative contribution of this component, compared to the bremsstrahlung and π^0 -decay gamma-rays from specific dense regions is significantly reduced because of the enhanced gas density. Following Aharonian & Atoyan 2000 in Fig.5 we show the contribution to the emission due to IC scattering of background electrons to the emission spectra. The ratio of luminosities from non-thermal bremsstrahlung to hadronic γ -rays does not depend on the ambient gas density. However, the contribution of the bremsstrahlung of background electrons to the total diffuse emission above 1 GeV is rather low, so it can be ignored.

When CRs interact with ambient matter through inelastic collisions they produce not only neutral pions, but also charged pions. These charged pions decay into secondary electrons, positrons and neutrinos (see Gabici, Aharonian & Casanova 2009). Thus, in addition to the γ -ray emissivity due to neutral pion decay, there will be a simultaneous radio synchrotron component due to the secondary electrons and positrons produced concomitantly with the neutral pions. The secondary leptons will also produce γ -ray emission through bremsstrahlung and inverse Compton. However, as discussed in Gabici, Aharonian & Casanova 2009 , the contribution of bremsstrahlung and inverse Compton of secondary leptons is negligible and the pion decay emission is dominant in the large energy range from GeV to TeV energies, assuming for the protons the energy spectrum given by Eq.8. The radio emission of primary and secondary electrons in the environments surrounding SNRs is of interest, but is beyond the scope of this paper and will not be discussed here.

4. Results and discussion

4.1. *The emission of background CRs*

We first calculate the spatial features of the hadronic γ -ray emission under the assumption that the CR spectrum in the region of longitude range $340^\circ < l < 350^\circ$ and latitude range $-5^\circ < b < 5^\circ$ is uniform and equal to the locally observed CR flux. Figure 2 shows the γ -ray emission from this region arising from the interactions of background CRs, whose spectrum is given in Eq.8, with the ambient atomic and molecular hydrogen, as measured by the LAB

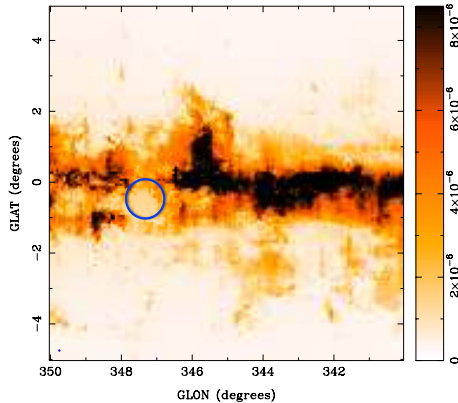


Fig. 2. The γ -ray energy flux arising from the background CRs, expressed in $\text{GeV cm}^{-2} \text{sr}^{-1} \text{s}^{-1}$ at 1 TeV. The blue ring represents a sphere of 10 pc radius around the location of the SNR RX J1713.7-3946 (the radial extension of the radio SNR shell).

and NANTEN surveys. The background CR spectrum being uniform, the morphology of the emission reproduces the gas distribution and does not change with energy. In Figure 2 the emission at 1 TeV is plotted. The blue ring represents a sphere of 10 pc radius (the radial extension of the radio SNR shell) around the location of the SNR RX J1713.7-3946. Hereafter we assume that the CR spectrum within 10 pc radius from RX J1713.7-3946 is equal to the CR background spectrum, since we are interested in the emission of CRs leaving their injection source and not in the emission produced by the injected CRs within the SNR shell.

4.2. The emission of background and runaway CRs

Figure 3 shows the predicted hadronic γ -ray emission at 1 TeV arising from the sum of background CRs and the runaway CRs (i.e., $\rho_{bg} + \rho_{SNR}$) as given by Eq. 7 for the diffusion coefficients discussed in Section 3. The spatial distribution of the emission depends upon the CR diffusion coefficient, D_0 . The faster the CRs diffuse into the ISM, the further the enhanced emission extends beyond the linear extent of RX J1713.7-3946. However, for very fast diffusion ($D_0 = 10^{28} \text{ cm}^2/\text{s}$) the VHE runaway protons have already left the region around the SNR. The shape of the emission depends also upon the assumptions concerning the SNR injection history. We have namely assumed that the SNR, which is now about 1600 years old, has started to inject the most energetic particles at $t_{Sedov}=100$ years after the explosion. According to Eq.2 this assumption means that nowadays the SNR starts releasing CRs of energy about 100 TeV. CRs of energy lower than 100 TeV are still confined in the SNR shell, whereas higher energy particles have already left it. The γ -ray emission produced by a proton of 100 TeV peaks at around 10 TeV. Roughly speaking, CRs of a given energy are responsible for hadronic γ -ray emission which is about 10 times less energetic. The assumption that CRs of energy below 100 TeV are still confined in the SNR shell means then that one expects to observe almost no γ -ray enhanced emission due to runaway protons at energies below few TeVs in the surroundings of the SNR RX J1713.7-3946. The assumption on the injection history of the CR

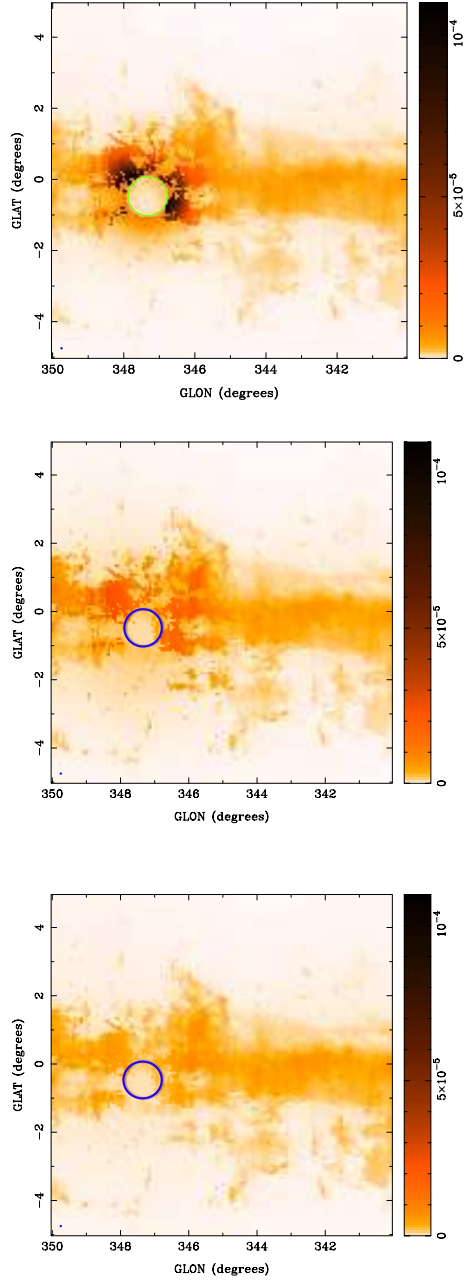


Fig. 3. The predicted hadronic γ -ray energy fluxes at 1 TeV, expressed in $\text{GeV cm}^{-2} \text{sr}^{-1} \text{s}^{-1}$, arising from background CRs and from CRs escaping the SNR shells if the CR diffusion coefficient, D_0 , is equal to $10^{26} \text{ cm}^2/\text{s}$ (upper panel), $10^{27} \text{ cm}^2/\text{s}$ (middle panel) and $10^{28} \text{ cm}^2/\text{s}$ (bottom panel). We assume that the SNR has started releasing the particles of energy 500 TeV 100 years after the explosion. Also indicated in the left bottom corner the angular resolution of the NANTEN survey.

source is therefore crucial to determine the spatial and spectral features of the γ -ray emission.

One would expect that the γ -ray emission from MCs illuminated by the CRs injected from nearby CR sources is spatially correlated with the atomic and molecular gas distribution. This is, generally speaking, true. However, one has to take into account that both the acceleration history of the source and the diffusion timescale are processes dependent upon the energy. In other words, when considering γ -ray emission at a given energy from the region surrounding a SNR, one should expect a correlation between hadronic γ -ray and the gas distribution if and only if the parent CRs have already been released by the SNR and had time enough to diffuse into the ISM. On the other hand, the environment of a CR source, which is dense in atomic and molecular hydrogen, might nonetheless appear faint at some energies in γ -rays simply because the parent CRs have not escaped the injection source or have not had time enough to propagate throughout the region nearby the source.

Figure 4 shows the average CR energy density from four different regions of 0.2×0.2 degrees around the positions a = (346.8, -0.4), b = (346.9, -1.4), c = (347.1, -3.0) and d = (346.2, 0.2). The CR energy density from these four regions is averaged over 200 parsecs around 1 kpc along the line of sight distance. If averaged over the whole line of sight distance from 50 parsecs to 30000 parsecs the CR energy density would be dominated by the energy density of the background. The background CR energy distribution is also shown in each panel a, b, c and d of Figure 4 for comparison. The CR energy distributions in the panels a, b, c and d, corresponding to the different locations and plotted for different diffusion coefficients D_0 , vary depending upon the location and the diffusion coefficient. The average gas density in the four regions a,b,c and d is about 3, 1, 1 and 8 protons/cm³, respectively. The total mass in solar masses, M_\odot , contained in these four regions is 458, 100, 88 and 1013 M_\odot for distances between 900 and 1100 parsecs.

Figure 5 shows the γ -ray spectra from regions a,b,c and d if one considers the hadronic emission produced along the line of sight distance between 900 and 1100 parsecs (in dashed lines) and the hadronic emission obtained by summing the radiation contributions over the whole line of sight distance (in solid lines). The contribution to the emission from inverse Compton scattering of background electrons, obtained following the modeling of Aharonian & Atoyan 2000, is indicated with a dashed light blue line. In all four locations the hadronic γ -ray emission is enhanced with respect to the hadronic emission due only to background CRs at energies above few TeVs as a consequence of the fact that the CR fluxes are enhanced above 100 TeV. The hadronic γ -ray emission from the region d is particularly enhanced with respect to the hadronic emission from background CRs. This is due to two factors, the enhanced CR flux nearby the injection source and the high ambient gas density. In the three regions a, b and d the high energy emission is clearly dominated by the radiation produced along the line of sight distance between 900 and 1100 parsecs, plotted in dashed lines in Figure 5. The γ -ray emission from high latitude regions, such as region c, is instead dominated by the contribution from

IC scattering of background electrons, almost at all energies. In regions closer to the Galactic Plane the emission from inverse Compton scattering of background electrons is subdominant at TeV energies, where runaway cosmic rays produce the enhanced emission. Therefore the regions where to look for the emission from runaway particles are low latitude regions of higher gas density.

The γ -ray spectra show a peculiar concave shape, being soft at low energies and hard at high energies, which, as discussed in Gabici, Aharonian & Casanova 2009, might be important for the studies of the spectral compatibility of GeV and TeV gamma ray sources. The peculiar spectral and morphological features of the γ -ray due to runaway CRs can be therefore revealed by combining the spectra and γ -ray images provided by the Fermi and Agile telescopes at GeV and by present and future ground based detectors at TeV energies. As shown by the surveys of the Galaxy, published by Fermi at MeV-GeV energies (Abdo et al. 2009a), by HESS at TeV energies (Aharonian et al. 2005; Aharonian et al. 2006) and at very high energies by the Milagro Collaboration (Abdo et al. 2007; Abdo et al. 2009b), the various extended Galactic sources differ in spectra, flux and morphology. However, there is growing evidence for the correlation of GeV and TeV energy sources (Funk et al. 2008; Abdo et al. 2009b). These sources appear often spectrally and morphologically different at different energies, possibly due not only to the better angular resolution obtained by the instruments at TeV energies, but also to the energy dependence of physical processes, such as CR injection and CR diffusion. For this reason it is important to properly model what we expect to observe at different energies by conveying in a quantitative way all information by recognizing that the environment, the source age, the acceleration rate and history, all play a role in the physical process of injection and all have to be taken into account for the predictions.

Figure 6 shows the ratio of the hadronic gamma-ray emission due to total CR spectrum to that of the background CRs for the entire region under consideration. In our modeling only CRs with energies above about 100 TeV have left the acceleration site and the morphology of the emission depends upon the energy at which one observes the hadronic gamma-ray emission. The different spatial distribution of the emission is also due to the different energy-dependent diffusion coefficients, assumed in the three different panels.

As discussed at length in Paper 1 the distance to the molecular and atomic gas is highly uncertain. The principle uncertainty in the determination of the distance, which especially at distances close to the Sun, is as large as 2 kpc, comes from errors in the accuracy of the estimates of radial velocity of gas clouds. Uncertainties in the distance estimates affect also the determination of the conversion factor X in Eq. 1 (Arimoto et al. 1996), by which the emissivity of the CO line is converted to ambient matter density, and the determination of the number density of H_2 molecules from the measured CO intensity. As noted in Paper 1, these uncertainties do not affect the model predictions of the hadronic gamma-ray flux. This is because the hadronic gamma-ray emissivity is proportional to the gas mass and inversely

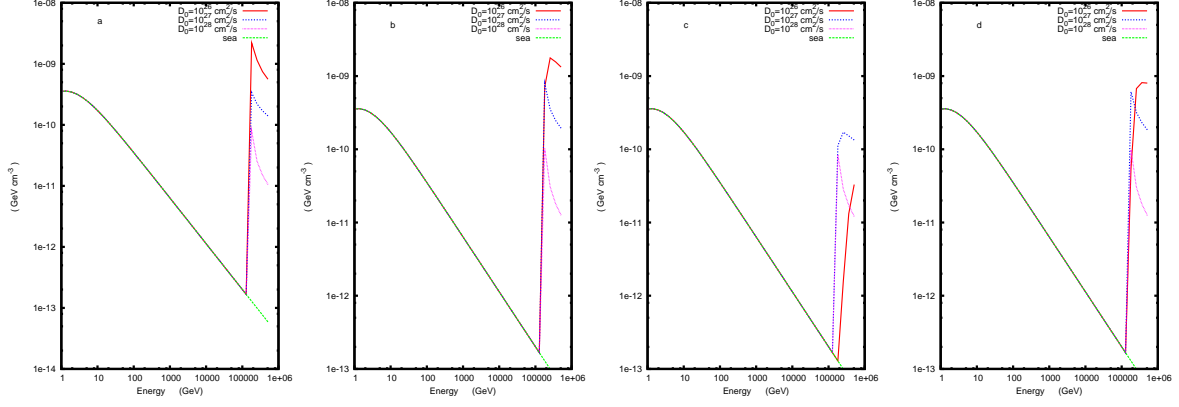


Fig. 4. The average CR proton energy density in four different regions of 0.2×0.2 degrees around the positions a = (346.8, -0.4), b = (346.9, -1.4), c = (347.1, -3.0) and d = (346.2, 0.2). The CR density is averaged over 200 parsecs around 1 kpc along the line of sight distance. The CR energy distributions in the panels a,b,c and d, corresponding to the different locations, are plotted for different diffusion coefficients D_0 . The background CR distribution is also shown in each panel for comparison.

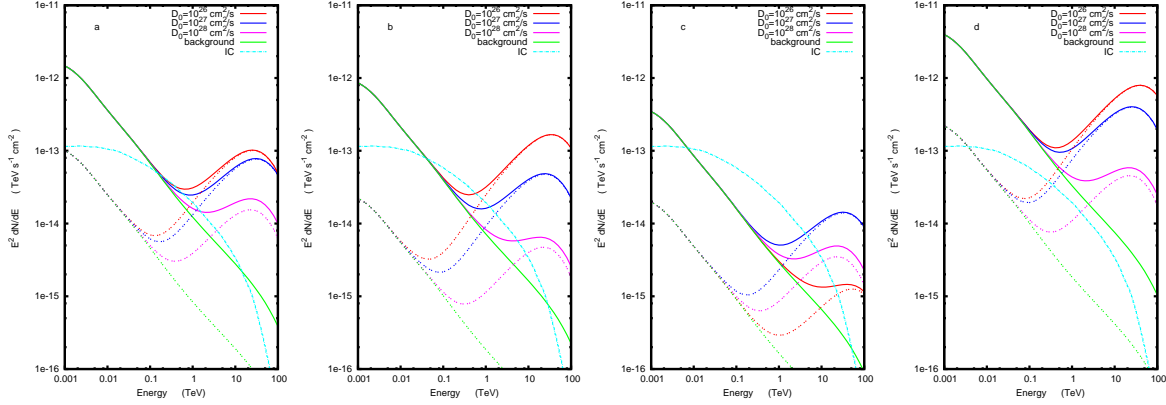


Fig. 5. The γ -ray energy flux in four different regions of 0.2×0.2 degrees around the positions a = (346.8, -0.4), b = (346.9, -1.4), c = (347.1, -3.0) and d = (346.2, 0.2). The emission produced along the line of sight distance between 900 and 1100 parsecs is plotted in dashed lines, while the emission obtained by summing the radiation contributions over the whole line of sight distance, from 50 parsecs to 30000 parsecs, is shown in solid lines. The emission in the panels a,b,c and d, corresponding to the different locations, is plotted for different diffusion coefficients D_0 . The emission from background CRs is also shown in each panel for comparison. The contribution to the emission from inverse Compton scattering of background electrons is indicated with a dashed light blue line. For the modeling of the inverse Compton contribution we follow Aharonian & Atoyan 2000 .

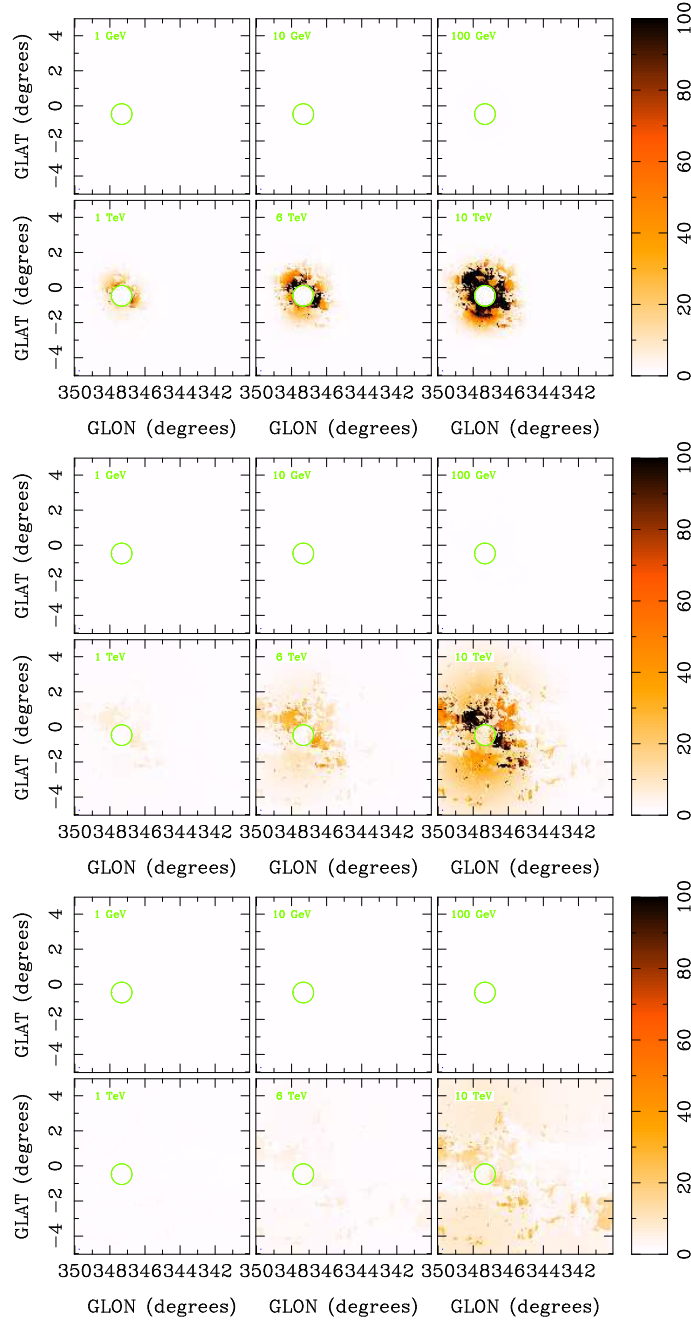


Fig. 6. Ratio of the emission due to the sum of background CRs and runaway CRs and background CRs only. The SNR is supposed to have exploded at 1 kpc distance from the Sun at 347.3° longitude and -0.5° latitude 1600 years ago and to have started injecting the most energetic protons 100 years after the explosion. The diffusion coefficient assumed within the region $340^\circ < l < 350^\circ$ and $-5^\circ < b < 5^\circ$ is 10^{26} cm^2/s in the upper panel, 10^{27} cm^2/s in the middle panel and 10^{28} cm^2/s in the bottom panel. In the three panels the ratio of the emission is shown for different energies from 1 GeV to 10 TeV.

proportional to the distance squared so that the relative errors exactly cancel.

5. Conclusions

CRs escaping SNRs diffuse into the ISM and collide with the ambient atomic and molecular gas. From such collisions γ -rays are created, which can possibly provide the first evidence of the parent population of runaway CRs. The γ -ray radiation from such hadronic interactions from regions close to CR sources depends not only on the total power emitted in CRs by the sources, and on the distance of the source to us, but also on the ambient interstellar gas density, the local diffusion coefficient and the injection history of the CR source. Due to the fact that the emission from gas clouds surrounding SNRs, illuminated in gamma-rays, depends upon many factors, it is difficult to draw strong conclusions about the nature of such emission. In order to test the standard scenario for CR injection in SNRs and CR propagation, we have computed the expected hadronic gamma-ray emissivity for the region $340^\circ < l < 350^\circ$ and $-5^\circ < b < 5^\circ$, assuming that a SN event has occurred in the location of the historical SNR RX J1713.7-3946 in 393 C.E.. Detailed modeling of the energy spectra and of the spatial distribution of the gamma-ray emission using the data from atomic and molecular hydrogen in the environment surrounding RX J1713.7-3946 have been presented. These predictions have shown that the age and acceleration history of the SNR, the particle diffusion regime and the distribution of the ambient gas are all paramount. The emission from the regions surrounding SNR shells can therefore provide crucial informations on the history of the SNR acting as a CR source and important constraints on the highly unknown diffusion coefficient. Also, depending on the time and energy at which one observes the remnants and the surrounds, one will observe different spectra and morphologies. This has important implications for the current and future generations of gamma-ray observatories. The high sensitivity and high resolution, which will be reached by future detectors, such as AGIS, CTA and HAWC (e.g. see reviews (Aharonian, Buckley, Kifune and Sinnis 2008 ; Hinton & Hofmann 2009)), makes the detection of the predicted emission possible.

6. Acknowledgements

Sabrina Casanova acknowledges the support from the European Union under Marie Curie Intra-European fellowships. The NANTEN telescope was operated based on a mutual agreement between Nagoya University and the Carnegie Institution of Washington. We also acknowledge that the operation of NANTEN was realized by contributions from many Japanese public donators and companies. This work is financially supported in part by a Grant-in-Aid for Scientific Research from the Ministry of Education, Culture, Sports, Science and Technology of Japan (Nos. 15071203 and 18026004, and core-to-core program No. 17004), JSPS (Nos. 14102003, 20244014, 18684003, and 22540250), and the Mitsubishi foundation.

References

- Abdo, A.A. et al, [Milagro Collaboration], 2007, ApJ, L664, 91
Abdo, A. A. et al, [Fermi Collaboration], 2009, ApJS, 183, 1, 46
Abdo, A. A. et al, [Milagro Collaboration], 2009, ApJ, 700L 127A
Abdo, A. A. et al, [Fermi Collaboration], 2009, ApJ, 706, L1
Abdo, A. A. et al, [Fermi Collaboration], 2010, Science, 327, 1103
Aharonian, F.A., Drury, L.O'C. & Völk,H.J.,1994, A&A, 285, 645
Aharonian, F. A. , 1991, Astrophysics and Space Science 180, 305
Aharonian, F. A. and A. M. Atoyan, 1996, A&A, 309, 917
Aharonian, F. A. and A. M. Atoyan, 2000, A&A, 362, 937
Aharonian, F. A. et al, [H.E.S.S. Collaboration], 2005, Sci, 307.1938A
Aharonian, F. A. et al, [H.E.S.S. Collaboration], 2006, ApJ636, 2, 777
Aharonian, F. A. et al., [H.E.S.S. Collaboration], 2006, Nature439, 695
Aharonian, F. A. et al., 2008, A&A481, 401
Aharonian, F. A. et al., 2008, A&A483 509
Aharonian, F. A. et al., 2008, A&A490 685
Aharonian, F., Buckley, J., Kifune, T., Sinnis, G., 2008, Reports on Progress in Physics, 71, 9, pp. 096901
Albert et al, ApJ664 87
Albert et al., A&A474 937
Arimoto,N., Sofue, Y. and Tsujimoto, T., 1996, PASJ, 48, 275A
Blandford, R. & Eichler, D., 1987, Phys. Rep.154, 1
Caprioli, D., Amato, E., Blasi, P., arXiv:0912.2964
Casanova, S. et al, 2009, PASJ (in press), arXiv:0904.2887v2
Castro, D. & Slane, P., 2010, arXiv1002.2738C
Dermer, C., 1986, A&A157, 223
Drury, L.O'C., Aharonian, F.A. & Völk, H.J.,1994, A&A287, 959
Fukui, Y. et al., 1999, PASJ, 51, 6
Fukui, Y. et al., 2001, PASJ, 53, 6
Fukui, Y. et al, 2003, ASPC, 287, 360
Fukui, Y. et al., 2008, e-Print:arXiv:0810.5416
Funk, S., et al, 2008 ApJ679, 1299F
Gabici, S., Aharonian, F. A., & Blasi, P., 2007, Astrophysics and Space Science, 309, 1-4, 365
Gabici, S. and Aharonian, F. A., 2007, ApJL665, 131
Gabici, S., Aharonian, F. A., & Casanova, S., 2009, MNRAS 396, 3, 1629
Issa, M. R. and Wolfendale, A. W., 1981, Nature, 292, 5, 430-433
Jones, D. I., Crocker, R. M., & Protheroe, R. J., 2008, PASA, 25, 161.
Jones, D. I., Crocker, R. M., Ott, J., et al., AJ submitted

Hinton, J. A. & Hofmann, W., Annual Review of Astronomy & Astrophysics, 47, 1, 523-565
Kamae, T. et al., 2006, ApJ, 647, 692
Kalberla, P.M.W., Burton, W.B., Hartmann, Dap, Arnal, E.M., Bajaja, E., Morras, R., and Pöppel, W.G.L., 2005, A&A440, 775.
Kelner, S.R., Aharonian F. A. & Bugayov, V.V., 2006, Phys ReV D 74, 034018
Lagage, P. O. & Cesarsky, C. J., 1983,A&A125, 249L
Mizuno,A., and Fukui, Y. 2004, ASP Conf. Proc., 317, 59.
Malkov, M. A. & O’C Drury,L., 2001, Reports on Progress in Physics, Volume 64, 4, 429
Montmerle, T., 1979, ApJ231, 95
Montmerle, T., 2009, Conf. "High-Energy Phenomena in Massive Stars", Jaen (Spain), Feb. 2-5, 2009
Mori,M., 1997, ApJ, 478, 225
Mori,M.,2009, APh, 31, 341M
Nakanishi, H. & Hiroyuki, S., 2003, PASJ, 55, 191.
Nakanishi, H. & Hiroyuki, S., 2006, PASJ, 58, 847.
Particle Data Group, 2008, Phys. Lett. B, 667, 212.
Paul, J., Casse, M. and Cesarsky, C. J., 1976, ApJ, 207, 62
Ptuskin, V.S. & Zirakashvili, V.N. 2005, A&A 429, 755
Protheroe, R. J., Ott,J., Ekers, R. D., et al., 2008, MNRAS 390, 683.
Rodriguez Marrero, Ana Y., Torres, Diego F., de Cea del Pozo, Elsa, Reimer, Olaf, Cillis, Anala N., 2008, ApJ689, 213R
Tavani, M. et al, 2010, ApJ710, L151
Uchiyama, Y., Aharonian, F. A., Tanaka, T. Takahashi, T. & Maeda, Y., 2007, Nature 449, 576U
Zirakashvili, V.N. & Ptuskin, V.S., 2008, ApJ, 678, 939
Wang, Z. R., Qu, Q. Y. & Chen, Y., 1997 A&A318, L59